

# Towards bicycle demand prediction of large-scale bicycle sharing system

Yufei HAN\*      Latifa Oukhellou†      Etienne Come‡

**Submitted For Publication**  
**93rd Annual Meeting of the Transportation Research Board**  
**January 12, 2014**

## **Word Count:**

Number of figures:	6 (250 words each)
Number of tables:	1 (250 words each)
Number of words in texts:	4821
Total:	$4821 + 7 * 250 = 6571$ (MAX 7500)

---

\*Corresponding Author, IFSTTAR/GRETTIA, France, [yfhan.hust@gmail.com](mailto:yfhan.hust@gmail.com)

†IFSTTAR, [latifa.oukhellou@ifsttar.fr](mailto:latifa.oukhellou@ifsttar.fr)

‡IFSTTAR, [etienne.come@ifsttar.fr](mailto:etienne.come@ifsttar.fr)

## Abstract

We focus on predicting demands of bicycle usage in Velib system of Paris, which is a large-scale bicycle sharing service covering the whole Paris and its near suburbs. In this system, bicycle demand of each station usually correlates with historical Velib usage records at both spatial and temporal scale. The spatio-temporal correlation acts as an important factor affecting bicycle demands in the system. Thus it is a necessary information source for predicting bicycle demand of each station accurately. To investigate the spatio-temporal correlation pattern and integrate it into prediction, we propose a spatio-temporal network filtering process to achieve the prediction goal. The linkage structure of the network encodes the underlying correlation information. We utilize a sparsity regularized negative binomial regression based variable selection method to learn the network structure automatically from the Velib usage data, which is designed to highlight important spatio-temporal correlation between historical bicycle usage records and the bicycle demands of each station. Once we identify the network structure, a prediction model fit well with our goal is obtained directly. To verify the validity of the proposed method, we test it on a large-scale record set of Velib usage.

# 1 Introduction

Urban shared-mobility has attracted more and more attentions for both academic researchers and city policy-makers to build livable and sustainable communities. Bicycle sharing systems (BSS) have been very successfully deployed in many metropolitans in the world. The main motivation is to provide users with free or rental bicycles especially suited for short-distance trips in urban areas, thus reduces traffic congestion, air pollution and noise that leads to high economical and social cost. In Europe, BSSs are most popular in southern European countries. Thanks to their unquestionable success [7, 4], more and more European cities works to provide this mode of mobility in order to modernize the city planning. In France, the first implementation of BSS was in Lyon in 2005 (it is called Velib’v). Nowadays, BSSs have been launched in twenty French cities, including Paris, one of the most large-scale BSSs in France (it is called Velib).

The fundamental issue of BSS study is to understand bicycles mobility patterns and regulate availability of the bicycles in the urban network. Due to differences between city blocks in social activities and functions, demands of short-distance trips usually form non-uniform spatio-temporal patterns. Some BSS stations tend to face large demand of bicycles during specific time periods. The planning department of BSS thus needs to forecast the bicycle demand variations at each station, in order to balance the bicycle loading in the system. Several studies [10, 2, 16, 13] have shown the usefulness of analyzing the data collected by BSSs operators. The redistribution of bicycles can benefit from the analysis of statistical bicycle usage patterns [8, 14, 1].

Fruitful progress as these studies have achieved, there is still an open question of BSS service demand prediction. What are the factors affecting bicycle demands of one specific station ? How do the bicycle demands of one station correlate with historical bicycle usage patterns ? Previous works attacked the prediction of BSS demands mainly from two aspects. In [11], the spatio-temporal bicycle usage patterns of the whole network are extracted from BSS data using clustering algorithms and historical average of BSS demands corresponding to each pattern is employed to achieve the forecast goal. On the other hand, [11] ignores the spatio-temporal correlation and construct station-wise forecast only depending on the temporal dynamics of each station. However, both of them don’t investigate the spatio-temporal factors of bicycle demands with respect to individual stations explicitly.

The contribution of this paper aims at solving the investigation of the spatio-temporal bicycle usage patterns through a network structure learning procedure. Our objective is to exhibit the important factors affecting the Velib service demands at each station in order to provide a direct solution to the open problem. Based on the analysis, we are able to achieve our goal of Velib service demand forecast for the whole network immediately.

This paper is organized as follows. In Section.2, a general description of Velib system is given. Section.3 describes the proposed analysis methodology performed on the collected Velib usage data. Section.4 is devoted to illustrate the identified spatio-temporal factors on Velib service demand at each station. Section.5 presents the capabilities of the proposed method in forecasting Velib service demands, in comparison

45 with two other baseline regression technologies utilizing no explicit spatio-temporal  
46 factors of bicycle demands at all. Section.6 concludes the whole paper.

## 47 2 Velib system description

48 Velib is designed to facilitate sightseeing and public transportation in urban areas  
49 of Paris in 2007. Total 7,000 bicycles are initially distributed to 750 fixed stations.  
50 In 2008, Velib system is further extended to 20,000 bicycles over 1,208 fixed service  
51 stations. The system serves 110,000 short-distance trips on average per day. Most  
52 Velib stations are located within Paris. A small proportion of stations are distributed  
53 in the near suburbs in order to extend sharing service.

54 Velib provides a non-stop 24-hour bicycle rental service. Each Velib station has  
55 an automatic rental payment terminal and 8 to 70 bicycle docking positions. There  
56 are totally 40,000 docking positions available in the system. Each bike is locked to its  
57 docking position electrically. Users can either purchase a short-term (daily or weekly)  
58 usage of the bicycle or charge a annual pass card. To fetch the bicycle, the user need to  
59 show his usage card to RFID terminals equipped with each docking position in order to  
60 unlock the bicycle. The first 30 minutes for short-term rental and the first 45 minutes  
61 for annual rental of every trip is free of charge. Users can return the bicycles easily to  
62 any station at any time.

63 The Velib usage dataset used in our work is composed of over 2,500,000 trip records  
64 during five months (April, June, September, October, December) in 2011. To obtain  
65 stable usage patterns, we remove trips with time duration of less than one minute and  
66 with the same station as origin and destination from the data set. These fake trips  
67 correspond to users' mis-operations. Finally we reserve trips from 1188 stations in the  
68 city. Based on the trip data, we count the number of bicycles departing from and enter-  
69 ing each station per hour. The number of departing bicycles per hour at each station  
70 represents the hourly profile of Velib service demand at this station. Figure. 1 shows  
71 the histogram of time duration of each bicycle trip. The  $y$  axis represents the number  
72 of the trips with different levels of time duration length. Most trips are finished within  
73 less than 2 hours, which is consistent with the fact that Velib system serves the short-  
74 distance mobility in the city. We count the average number of departing bicycles per  
75 hour for all the stations to evaluate activity level of Velib usage globally in the system.  
76 Figure. 2 shows the difference in hourly Velib usage between weekdays and weekends.  
77 A cyclostationarity pattern can be seen in Velib usage during weekdays. Three peaks  
78 of weekday usage can be observed in Figure 2: the most significant two correspond to  
79 the public commutes (from 8am to 10am and from 6pm to 9pm), while the third one  
80 from 11 am to 13 pm corresponds to the lunch break. They represent travel patterns of  
81 public transportation, such as home-office and office-restaurant patterns. In contrast,  
82 the morning peak usage disappears during the weekends. Velib usage gradually reaches  
83 the maximum in the afternoon, reflecting the travel patterns of the leisure time.

84 These statistics give a general profile of Velib usage patterns in the system. In  
85 this paper, based on the extracted Velib usage count data, we aim to achieve short-  
86 term forecast of the bicycle demands at each station by analyzing inter-station spatio-  
87 temporal correlation of bicycle usages.

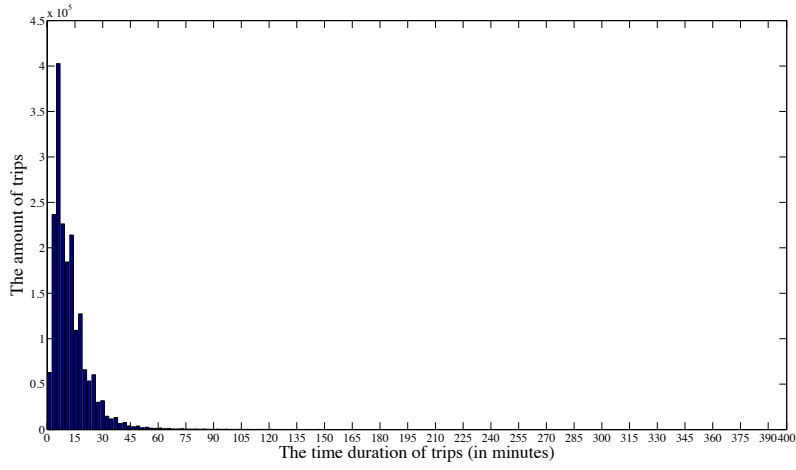


Figure 1: Statistics of time duration of each trip

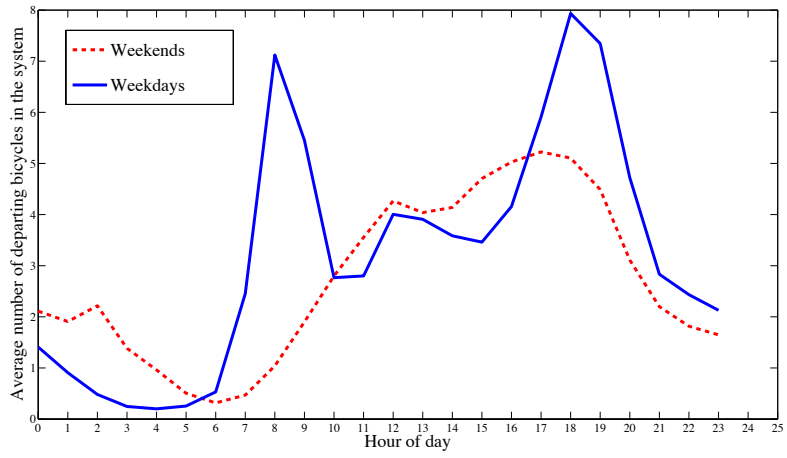


Figure 2: Average number of departing per hour during weekdays (continuous blue line) and weekends (dashed red line).

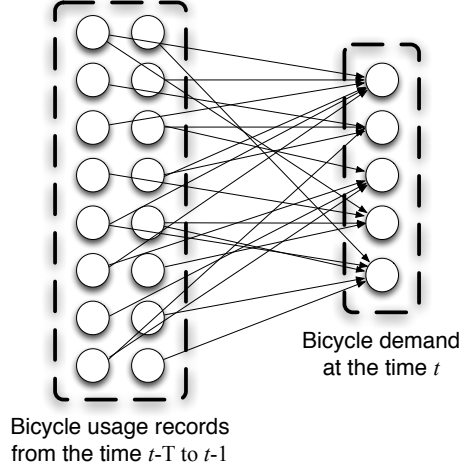


Figure 3: Spatio-temporal predictive network

### 3 Velib demand prediction through learning of spatio-temporal network structure

We use  $X_{i,t}^{out}$  and  $X_{i,t}^{in}$   $i = 1, 2, 3, \dots, n$  to note the number of bicycles departing from and entering the station  $i$  at the time  $t$  respectively.  $n = 1188$  is the number of Velib stations. Each pair of  $X_{i,t}^{out}$  and  $X_{i,t}^{in}$  indicate the temporal dependent usage pattern of Velib service of each station. Notably  $X_{i,t}^{out}$  represents bicycle demands of the station  $i$  at the time  $t$ , which is the target of the predictive analysis. In our work, we assume that the temporal dynamics of bicycle demand is a stationary markov process. It means the  $X_{i,t}^{out}$  only depends on the recent Velib usage records from  $t - T$  to  $t - 1$ . Considering most Velib trips are short-distance travels that last no more than 2 hours, the markovian assumption is reasonable and we set  $T$  to be 2. With this setting, the conditional dependence between historical Velib usage records and the bicycle demands to be predicted in the system can be described using a spatio-temporal network  $G = \{\Delta_1, \Delta_2, E\}$ , as in Figure. 3.  $\Delta_1$  and  $\Delta_2$  are two sets of nodes. Each node of  $\Delta_1$  is the historical Velib usage  $X_{i,j}^{out}$  and  $X_{i,j}^{in}$  in the system from the time  $j = t - T$  to  $j = t - 1$ . Nodes of  $\Delta_2$  correspond to bicycle demands at the time  $t$   $X_{i,t}^{out}$  for each station, which are the prediction target.  $E$  is the set of directed edges linking nodes of  $\Delta_1$  and  $\Delta_2$ . The linkage structure of the network represents spatio-temporal correlations between the historical Velib usage records  $X_{i,j}^{out}$  and  $X_{i,j}^{in}$  ( $i = 1, 2, 3, \dots, n, j = t - T, t - T + 1, \dots, t - 1$ ) and the prediction target  $X_{i,t}^{out}$  ( $i = 1, 2, 3, \dots, n$ ).

A link from one node in  $\Delta_1$  to another in  $\Delta_2$  represents the existence of spatio-temporal correlation that is useful for prediction between the two nodes. On the contrary, if two nodes from different sets are separated with no linkage, they are irrelevant with respect to the prediction goal. The interior linkage between nodes within  $\Delta_1$  and  $\Delta_2$  are ignored since we aim to construct a prediction model instead of a generative model to simulate spatio-temporal dynamics of Velib usage.

115 For each node  $s$  in  $\Delta_2$ , we note the  $N(s)$  is the set of nodes in  $\Delta_1$  that are linked to  
 116 the node  $s$ . In the domain of network structured data analysis,  $N(s)$  is also defined as  
 117 a neighbor set of  $s$  in the network  $G$ . Identifying neighborhood structure for each node  
 118 in  $\Delta_2$  finally achieves to reconstruct the network structure. In our work, neighborhood  
 119 selection is the key step to analyze the useful spatio-temporal correlation between  $\Delta_1$   
 120 and  $\Delta_2$ . In statistics, it is an intuitive solution to calculate covariances between nodes  
 121 of  $\Delta_1$  and  $\Delta_2$  and judge the correlation level given the covariances. However, in large-  
 122 scale urban area, the number of nodes in  $\Delta_1$  ( $n$  times  $T$ ) is usually much larger than the  
 123 volume of the available historical Velib usage records. The derived covariances easily  
 124 generates fake correlation between nodes [9]. In machine learning research, estimating  
 125 correlation structure of high-dimensional data is a popular topic. Most solutions are  
 126 proposed by performing global sparsity constraint on covariance matrix of data to  
 127 find the strong correlation patterns [9]. This kind of methods assumes that all nodes  
 128 follow a joint normal distribution. It fits the joint data distribution with a generative  
 129 gaussian random field [9], which is beyond the goal of the prediction task. Furthermore,  
 130 the joint normal distribution assumption is not valid for count data. The alternative  
 131 solutions investigate the correlation of each node in the network with the others by  
 132 performing sparsity-inducing regression. Treating the concerned node  $s$  in  $\Delta_2$  as the  
 133 regression target and the other nodes in  $\Delta_1$  as covariate of regression, the sparsity-  
 134 inducing regression generates sparse regression coefficients. Zero coefficients indicate  
 135 conditional independence between the corresponding nodes of  $\Delta_1$  and the concerned  
 136 node  $s$ , while coefficients with distinctively large magnitudes indicate strong correlation  
 137 between them. Benefited from the regression-oriented neighborhood selection scheme,  
 138 the identified correlation structure is intrinsically selected to suit the prediction task.  
 139 Furthermore, we can obtain a prediction model immediately after fixing the network  
 140 structure. Therefore, we address the issue of network structure learning following this  
 141 idea.

### 142 **3.1 $L1$ -norm regularized negative binomial regression for** 143 **neighborhood selection**

144 For each node  $X_{\Delta_2,s}$  in  $\Delta_2$ , we identify its neighbors in  $\Delta_1$  with a sparsity regularized  
 145 regression model. The mathematical expression is defined as follows:

$$\begin{aligned}
 (\theta_k^s) &= \min_{\theta^s} f(X_{\Delta_2,s}, X_{\Delta_1,k}, \theta^s) + \lambda \|\theta^s\| \\
 k &= 1, 2, \dots, 2 * n * T
 \end{aligned}
 \tag{1}$$

146 In Eq 1,  $X_{\Delta_1,k}$   $k = 1, 2, \dots, 2 * n * T$  represents all nodes in  $\Delta_1$ , representing historical  
 147 records of the number of bicycles entering or departing from each station within the  
 148 time frame from  $t - T$  to  $t - 1$ .  $\theta^s$  is the regression coefficient vector of the same  
 149 dimension as  $X_{\Delta_1,k}$   $k = 1, 2, \dots, 2 * n * T$  for the station  $s$ . Each component  $\theta_k^s$  is the  
 150 regression coefficient for the corresponding node  $X_{\Delta_1,k}$ .  $\|\theta\|$  is the  $L1$  norm of  $\theta^s$ ,  
 151 defined as sum of absolute values of each  $\theta_k^s$ . The function  $f(X_{\Delta_2,s}, X_{\Delta_1}, \theta^s)$  is a  
 152 generalized linear regression model to suit different types of the regression target.  $\lambda$   
 153 is the penalty parameter balancing the sparsity-introducing regularization and the

154 regression cost. In [5, 15, 18],  $f$  is a least regression function on  $X_{\Delta_2,s}$  suited for  
 155 continuous variable. [17] defines  $f$  as a logistic regression function since the regression  
 156 target is a binary in Ising model. In our work,  $X_{\Delta_2,s}$  represent the number of bicycle  
 157 rented at the station  $s$ , which is integer count data. Therefore, we define  $f$  as negative  
 158 binomial regression model as in Eq 2.

$$f = \log P_{nb} \left( X_{\Delta_2,s} \right)$$

$$P_{nb} \left( X_{\Delta_2,s} \right) = \frac{\Gamma \left( X_{\Delta_2,s} + \psi \right)}{\Gamma \left( X_{\Delta_2,s} + 1 \right) \Gamma \left( \psi \right)} \left( \frac{\psi}{\psi + \mu} \right)^\psi \left( \frac{\mu}{\mu + \psi} \right)^{X_{\Delta_2,s}} \quad (2)$$

159 where  $\mu = e^{\sum_k \theta_k^s X_{\Delta_1,k}}$  is the mean of the negative binomial distribution  $P_{nb} \left( X_{\Delta_2,s} \right)$ .  
 160 In generalized linear model, it is fitted using the exponential link function based on the  
 161 covariate  $X_{\Delta_1,k}$ .  $\psi$  is the dispersion parameter of negative binomial distribution.  $\Gamma$  is  
 162 the Gamma function defined as  $\Gamma(n) = (n-1)!$ . Negative binomial regression [12] is a  
 163 generalized poisson regression to fit the dispersed count data with the larger variance  
 164 than the mean. The standard poisson regression is formulated as follows:

$$P_{poisson} \left( X_{\Delta_2,s} \right) = \frac{e^{-\mu_p} \mu_p^{X_{\Delta_2,s}}}{X_{\Delta_2,s}!} \quad (3)$$

165 where  $\mu_p = e^{\sum_k \theta_k^s X_{\Delta_1,k} + \varepsilon}$ , including a random intercept  $\varepsilon$  as random noise.  $\mu_p$  is the  
 166 product of the link function  $e^{\sum_k \theta_k^s X_{\Delta_1,k}}$  and the random factor  $\nu = e^\varepsilon$ . The link  
 167 function represents the non-linear relation between the poisson mean and the input  
 168 covariate. Negative binomial regression is then derived by performing gamma prior  
 169 probability on the random factor  $\nu$  and integrating out  $\nu$ , as expressed in the followings:

$$P_{nb} \left( X_{\Delta_2,s} \right) = \int_0^\infty P_{poisson} \left( X_{\Delta_2,s} \right) h(\nu) d\nu \quad (4)$$

170 where  $h = \frac{\delta^\psi}{\Gamma(\psi)} \nu^{\psi-1} e^{-\nu\delta}$  is the gamma prior probability on  $\nu$ .  $\delta$  is the shape parameter  
 171 of the gamma distribution. In poisson regression, both the mean and variance of poisson  
 172 distribution equals to  $\mu$ . However, in the Velib count data, the count data  $X_{\Delta_2,s}$  are  
 173 more dispersed. The variance is distinctively larger than the mean. By introducing  
 174 the gamma prior probability in Eq. 4, the mean and the variance of  $X_{\Delta_2,s}$  are modeled  
 175 respectively as  $\mu$  and  $\mu + \frac{\mu^2}{\psi}$  in negative binomial regression. The dispersion parameter  
 176  $\psi$  enables more flexibility to fit variance with different magnitudes. When  $\psi$  goes into  
 177 infinity, negative binomial regression is reduced to standard poisson regression.

178 Performing the  $L1$  norm based penalization leads to a sparse  $\theta^s$  vector. Only a small  
 179 proportion of components  $\theta_k^s$  have distinctively large magnitudes, while the others are  
 180 exactly zeros or have very small magnitudes approaching to zero. Through this way, the  
 181 nodes  $X_{\Delta_1,k}$  with distinctively large non-zero  $\theta_k^s$  are the most important spatio-  
 182 temporal factors affecting the bicycle demands  $X_{\Delta_2,s}$ . It indicates the existence of  
 183 linkage between the corresponding historical Velib usage records and  $X_{\Delta_2,s}$ . The weight  
 184 of this link is the value of the coefficient  $\theta_k^s$ . The rest extremely weak or zero coefficients

185 have no weight in predicting, thus they indicate no linkage connecting the corresponding  
186 nodes in  $\Delta_1$  to  $X_{\Delta_2,s}$ . The sparse structure of  $\theta^s$  gives rise to a compact spatio-temporal  
187 correlation structure in the network. Once we fix the network structure according to  
188  $\theta^s$ , it is then direct to construct a negative binomial regression model to predict  
189 the bicycle demands of the station  $s$ . Given all Velib historical usage information in  $\Delta_1$   
190 as input, the prediction for all 1188 stations proceeds as a network filtering procedure,  
191 providing estimation of nodes in  $\Delta_2$ . Discriminating power of this generalized linear  
192 model is verified in previous works [12]. The predictive model integrates the spatio-  
193 temporal correlation of Velib usage records. The sparse structure of the network linkage  
194 improves the model compactness by removing irrelevant Velib usage information. In  
195 [18, 17], Xu et al proves that the  $L1$  norm regularization gives the asymptotically  
196 correct estimation of neighborhood structure if the underlying neighborhood is sparse.  
197 In Velib service, the bicycle demand denotes the short-distance trip custom in Paris.  
198 The bicycle demands at one station are only correlated with those of a specific group  
199 of stations. Therefore, this characteristic implies a underlying sparse spatio-temporal  
200 correlation structure. The penalization parameter  $\lambda$  is fixed by cross-validation in the  
201 neighborhood selection procedure. It is chosen as the one that minimizes the regression  
202 error while reserving the sparsity of  $\theta$  in cross-validation.

### 203 3.2 Solution to regularized negative binomial regression

204 We assume the training data involves total  $m$  days of Velib usage data. Each day  
205 contains 24-hour records of  $X_{i,t}^{out}$  and  $X_{i,t}^{in}$   $i = 1, 2, 3, \dots, n, t = 1, 2, 3, \dots, 24$ . As a result,  
206 we can sample 22 time frames of length 2 to form the set  $X_{Delta_1}$  on each day. In  
207 this setting, we can construct a training data set containing  $22 * m$  pairs of  $X_{Delta_1,k}^j$   
208 ( $k = 1, 2, 3, \dots, 2 * n * T$ ) and  $X_{Delta_2,s}^j$  ( $j = 1, 2, 3, \dots, 22 * m$ ). The objective function for  
209 estimating  $\theta^s$  is then formulated as follows:

$$\theta^s = \min_{\theta^s} \sum_{j=1,2,3,\dots,22*m} f \left( X_{\Delta_2,s}^j, X_{\Delta_1}^j, \theta^s \right) + \lambda \|\theta^s\| \quad (5)$$

210 Given a fixed penalization parameter  $\lambda$ , minimizing the cost function in Eq. 5 with  $f$   
211 as the negative binomial regression equals to solve a regularized maximum likelihood  
212 problem. However,  $f$  is not convex due to simultaneous optimization with respect to  $\theta^s$   
213 and the dispersion parameter  $\psi$ . To address problem, an interior point optimization  
214 method [3] is applied to relax the original minimization procedure and search for an  
215 approximated solution. The basic idea is to optimize the cost function Eq. 5 with  
216 respect to only one variable at each time, while the other one is fixed. Each subproblem  
217 of optimization is convex and easy to solve by taking the first-order conditions and  
218 making them equal to zero. The two first-order optimum conditions, one for  $\theta$  and one

219

for  $\psi$ , are presented as:

$$\sum_{j=1,2,3,\dots,22*m} \frac{X_{\Delta_{2,s}}^j - \mu_j}{1 + \psi^{-1}\mu_j} + \text{sgn}(\theta^s) = 0$$

$$\sum_{j=1,2,3,\dots,22*m} \left( \frac{\log 1 + \psi^{-1}\mu_j - \sum_{l=1,2,3,\dots,X_{\Delta_{2,s}}^j-1} 1}{(\psi^{-1})^2} + \frac{X_{\Delta_{2,s}}^j - \mu_j}{\psi^{-1}(1 + \psi^{-1}\mu_j)} \right) = 0 \quad (6)$$

220

221

222

223

224

225

226

227

where  $\mu_j = e^{\sum_k \theta_k^s X_{\Delta_{1,k}}^j}$  and  $\text{sgn}$  indicates the signs of all  $\theta_k^s$  in  $\theta^s$ . Original difficult jointly optimizing problem is relaxed to alternative updates of the parameters  $\theta$  and  $\psi$  iteratively until convergence. Since the non-convexity of the cost function, the alternative update procedure doesn't guarantee to achieve a global optimum. A proper warm-start allows the alternative optimization procedure to achieve reasonably good solution fast. In our work, we follow the idea of [12] to use a poisson regression parameter to initialize  $\theta$  and  $\psi$  in Eq. 4. For each station, the convergence is achieved for each fixed  $\lambda$  after 50 iterations on average.

228

## 4 Spatial-temporal correlation structure of Velib usage

229

230

231

232

233

234

235

236

237

238

239

240

241

242

243

244

245

246

247

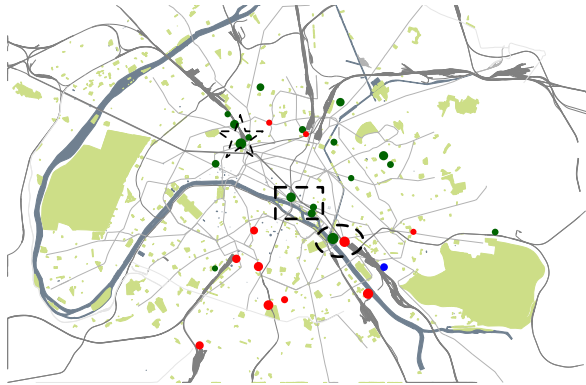
248

249

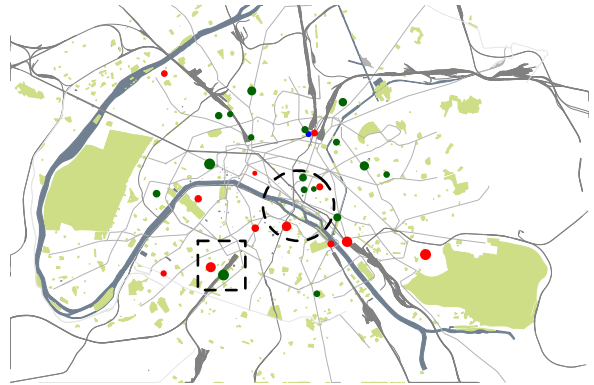
250

251

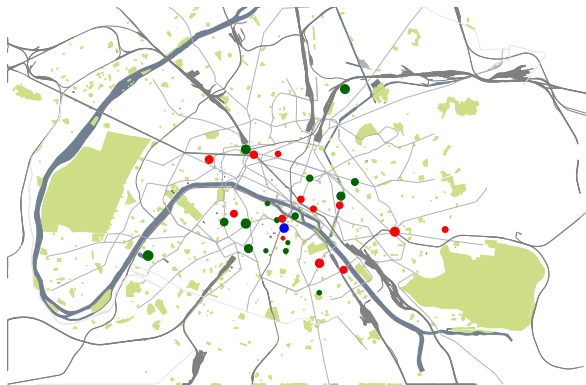
The sparse structure of the regression coefficients  $\theta^s$  indicates the historical Velib usage records  $X_{i,j}^{in}$  and  $X_{i,j}^{out}$  ( $j = t - 1, t - 2$ ) that are the most informative for the prediction task. It unveils the compact spatio-temporal correlation pattern with respect to the station  $s$ . Magnitudes of the non-zero regression coefficients are proportional to the correlation level of the corresponding historical Velib usage records with the prediction target. In the followings, we illustrate the learned spatio-temporal correlation structures for four stations. Two of them corresponds to Velib stocking points located around the rail-way stations in Paris (Gare du Nord and Gare de Lyon). The other two are located in the down-town area of Paris, near the places of interests (Saint German des Pres and Louvre). Geographical locations of these four stations are carefully selected. Velib usage records of these stations represent typical Velib usage patterns of common home-office travels and sightseeing-oriented travels in Paris. Most short-distance mobility in Paris belong to either of the two travels. For each station  $s$ , if the sparse regression coefficient  $\theta^s$  has less than 20 non-zero entries, we illustrate all the correlated historical Velib usage records corresponding to the non-zero regression coefficients. Otherwise, we select the correlated historical records corresponding to the 20 non-zero regression coefficients of the largest magnitudes. The blue pots in the figures illustrate the concerned station  $s$ . The red pots indicate the station  $i$  ( $i \in 1, 2, 3, \dots, 1188$ ) corresponding to selected  $\{X_{i,j}^{out}\}$  during the precedent 2 hours that are the most correlated with  $X_{s,t}^{out}$ , while the green pots are the the station  $i$  ( $i \in 1, 2, 3, \dots, 1188$ ) corresponding to the most correlated  $\{X_{i,j}^{in}\}$  during the precedent 2 hours.



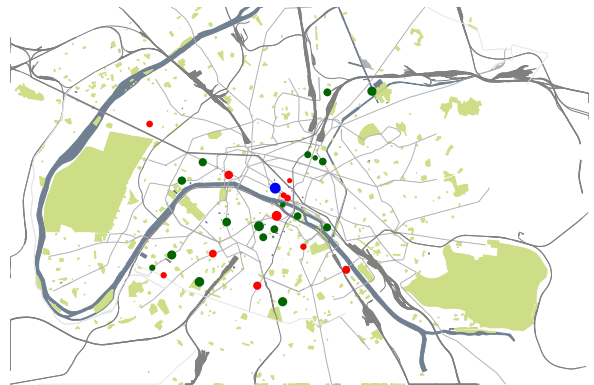
(a) Gare de Lyon



(b) Gare du Nord



(c) Saint Germain des Pres



(d) Louvre

Figure 4: Typical spatio-temporal correlation structure.

In Figure 4(a) and 4(b), we can find both local and non-local spatial-temporal correlation structures. For example in Figure 4(a), Velib service demand near Gare de Lyon is strongly correlated with historical Velib usage information at the entrance of Gare de Lyon (noted by a circular region) and Hotel de Ville (noted by a square region) that locates closely to Gare de Lyon. Besides, Velib usage records around Gare de Saint-Lazare (noted by a star-shaped legend) also present high-level correlation with the prediction target. In Figure 4(b), Velib demand at Gare du Nord has a non-local correlation with Velib usage records at Gare Montparnasse (noted with a circular legend) and the center of Paris (noted with a square legend). The existence of the spatio-temporal correlation doesn't necessarily indicate the existence of physical bicycles flows between the selected stations and the the concerned station  $s$ . It means that the historical Velib usage patterns at those stations provides the most critical information in prediction the Velib demand at the station  $s$ . This spatio-temporal correlation structure is arisen by either bicycle flow interactions or similar temporal dynamic patterns of Velib usage. The former presents a local correlation at most time and can be investigated further by looking into trip records, while the latter usually presents a non-local correlation structure and can not be captured by the trip data. It provides complementary information for prediction of Velib service demand at the concerned station. In Figure 4(c) and 4(d), the spatio-temporal correlation structure are more local than that in the first two figures, Most selected correlated stations locate within the neighborhood of the concerned station. This phenomenon represents the characteristics of sightseeing mobility patterns. Different from public transportation, Velib usages for sightseeing are concentrated near the places of interests of the city. In Paris, most places of interests are distributed near Boulevard de Saint-Germain des Pres and Musee du Louvre, along the Seine river. Therefore, originations and destinations of sightseeing travel by Velib are usually within the same area. Besides, temporal variation of bicycle usage for sightseeing is normally inconsistent with that of daily commute. Thus, the bicycle flow interaction becomes the most importation factor affecting the Velib usage patterns of the last two stations, which in turn gives rise to the local spatio-temporal correlation structure.

## 5 Experiments on spatio-temporal prediction of bicycle usage demand

In this section, we illustrate the prediction performance of the proposed method. In all 152 days of Velib usage count data, we choose each day in turn for testing regression performance and use all the others for learning the network linkage structure  $\theta^s$  ( $s = 1, 2, 3, \dots, 1188$ ). For the testing day, given Velib usage count of precedent 2 hours ( $t - 1$  and  $t - 2$ ), the task is to predict the bicycle demand  $X_{:,t}^{out}$  at the time  $t$  for all 1188 stations based on the learned  $\theta^s$ , where  $t = 1, 2, 3, \dots, 22$ . The obtained  $\theta^s$  ( $s = 1, 2, 3, \dots, 1188$ ) are directly used to estimate the mean value  $\mu$  of the negative binomial regression model in Eq. 2. The mean value  $\mu$  is the forecast of bicycle demands. The absolute error between the predicted bicycle demands for each station  $s$  at each time  $t$  is obtained during the testing process. The sample mean and sample variance

of the absolute errors are used to evaluate prediction accuracy.

We compare the proposed method with two other prediction schemes. The first one is an intuitive solution. It constructs a poisson regression model for each station independently to achieve temporal prediction, ignoring the spatio-temporal correlation of Velib usage unveiled in the last section. The input of the poisson model for the station  $s$  is the Velib usage data  $X_{s,j}^{in}$  and  $X_{s,j}^{out}$  ( $j = t - 2, t - 1$ ). The output is the bicycle demand  $X_{s,t}^{out}$  at the time  $t$ . The parameters of each poisson regression model are estimated using the quasi-newton optimization. We name it as station-wise poisson regression hereafter.

The other one is designed to make use of the spatio-temporal patterns of Velib usage in an inexplicit way, It combines nearest neighbor regression technologies and state space temporal dynamic model to achieve prediction of the bicycle demand at each station simulataneously [6]. In this method, we treat Velib usage count  $X_{:,t}^{in}$  and  $X_{:,t}^{out}$  for all stations at the time  $t$  as a multivariate vector  $Y_t$  of  $1188 * 2 = 2376$  dimensions, considering both the volume of bicycles enterring and departing from each station. Based on the training set of 151 days, we form a matrix  $Y^{\text{train}} \in R^{3624 * 2376}$  by integrating daily records of all 151 days into the sequence of hourly records of  $151 * 24 = 3624$  hours. Each row is defined as  $Y_t$  and the rows are arranged following the temporal order of all 151 days in the training set. We then employ Principle Component Analysis (PCA) to decompose the matrix  $Y^{\text{train}}$  and project each row  $Y_t^{\text{train}}$  to a low-dimensional subspace. We calculate the first  $k$  principle eigen vectors of  $Y^{\text{train}}$  corresponding to the largest spectrum energy. These principle eigen vectors form a projection matrix  $P \in R^{3624 * k}$ , with the eigen vectors arranged as column vectors. The  $k$ -dimensional projection  $\Phi_t^{\text{train}}$  of each  $Y_t^{\text{train}}$  is expressed as  $P^T Y_t^{\text{train}}$ . Through this way, we integrate the spatio-temporal Velib usage patterns within the short-term time frames into a compact  $k$ -dimensional projection subspace  $\Omega$ . During the testing procedure, for the testing day, we firstly project the Velib usage count  $Y_j^{\text{test}}$  at the time  $j = t - 2, t - 1$  to the  $k$ -dimensional space  $\Omega$  using the projection matrix  $P$ . After that, we calculate the distance in the projection space between the sequence  $\{\Phi_{j=t-2,t-1}^{\text{test}}\}$  and the sequences  $\{\Phi_{j=(l-1)*24+t-2,(l-1)*24+t-1}^{\text{train}}\}$  at the corresponding time frame ( $j = t - 2, t - 1$ ) of each day  $l$  in the training data set, in order to identify the  $p$  nearest neighbors of the testing day in the subspace  $\Omega$ . The distance measure between the sequences is defined as summation of cosine distance between the PCA projections:

$$Dis = \sum_{j=t-2,t-1} \frac{\left(\Phi_j^{\text{test}}\right)^T \Phi_{(l-1)*24+j}^{\text{train}}}{\|\Phi_j^{\text{test}}\|_{L_2} \|\Phi_{(l-1)*24+j}^{\text{train}}\|_{L_2}} \quad (7)$$

where  $\|\cdot\|_{L_2}$  denotes the  $L_2$  norm of vector. The bicycle demand  $X_{:,t}^{out}$  of all stations at the time  $t$  on the testing day is predicted as the average of the bicycle demands  $X_{:,t}^{out}$  at the corresponding time  $t$  of the  $p$  nearest neighboring days in the training set. The PCA projection conserves global characteristics of Velib usage over the whole network. Nearest neighbor searching in the PCA space considers similarity of spatio-temporal Velib usage patterns between the historical records and the testing sample. The final prediction is a linear combination of the historical bicycle demands with similar precedent spatio-temporal Velib usage pattern. This scheme achieves to predict

Table 1: Prediction accuracies of the three methods

Prediction method	Average prediction error	Variance of prediction error
Station-wise poisson regression	2.05	15.6
NN+PCA	1.47	3.80
The proposed method	1.45	3.65

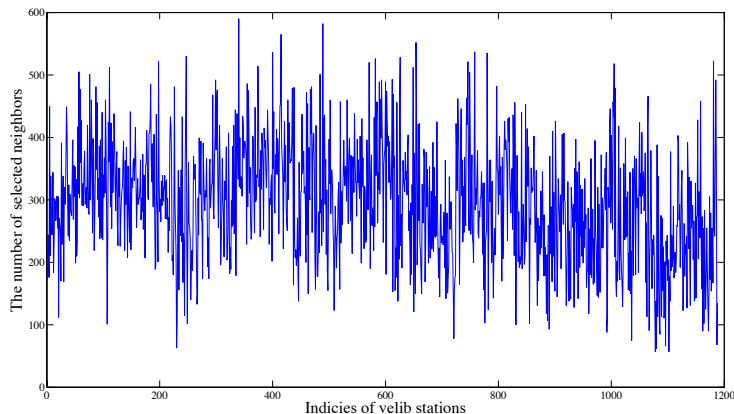
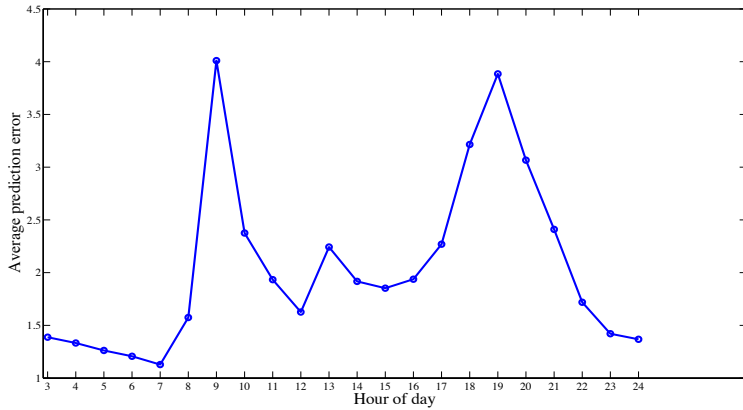


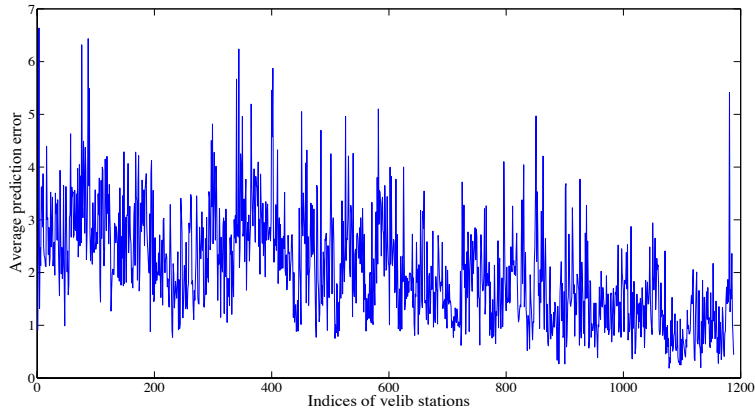
Figure 5: The number of selected neighbors for each station

336 the Velib demands at all stations simulatensouly. In the followings, we note this scheme  
 337 as  $NN + PCA$  for short. For fair comparison, we adjust the number of the nearest  
 338 neighbors in prediction to achieve the best performance.

339 As we can see in Table 1. The proposed negative binomial regression model achieves  
 340 superior performances to  $NN + PCA$  and the station-wise poisson regression model  
 341 with respect to both mean and variance of prediction error.  $NN + PCA$  performs  
 342 much better compared with the station-wise poisson regression. The experimental re-  
 343 sults are consistent with the original expectation. Both the proposed spatio-temporal  
 344 network based prediction method and the  $NN + PCA$  make full use of the short-  
 345 term spatio-temporal Velib usage patterns in constructing the temporal forecast model.  
 346 The station-wise poisson regression model only depends on station specific Velib us-  
 347 age records. The former two gains more predictive information from the investigated  
 348 spatio-temporal Velib usage patterns to narrow the variance of Velib demand estima-  
 349 tion, making the prediction more close to the underlying values. The network structure  
 350 learning procedure extracts the prediction-oriented spatio-temporal correlation struc-  
 351 ture with respect to each station. In contrast,  $NN + PCA$  conserves only global  
 352 spatio-temporal usage patterns. This global information is corase and is not tailored  
 353 for temporal prediction of each local station. Thus  $NN + PCA$  performs less accu-  
 354 rately than the proposed method. Figure 5 illustrates the the number of neighbors in  
 355  $X_{\Delta_2}$  for each station. As illustrated, the proposed method benefits from the sparsity-  
 356 introducing regularization to construct a sparse linkage structure in the spatio-temporal



(a) Average prediction error per hour



(b) Average prediction error per station

Figure 6: Hour-wise and station-wise average prediction error

357 network. 295 neighbors are selected for each station on average. This sparse linkage  
 358 structure is helpful in selecting the really useful spatio-temporal correlation of the Veilb  
 359 usage and improving the computational efficiency of prediction.

360 Figure 6(a) and Figure 6(b) illustrate the variation of average prediction error for  
 361 each hour and each station respectively by performing the proposed method in the  
 362 training/testing process. As shown in Figure 6(a), about ten percent of the all stations  
 363 has distinctively larger prediction errors than the others. They correspond to the  
 364 stations around transportation hubs, such as railway stations and places of interests in  
 365 Paris. Velib usage at those stations are easily affected by the social-economic factors,  
 366 such as type of the day (week-end, public holiday or common working days) and special  
 367 events (accidents or adjustment of public transportation modes). Figure 6(b) shows the  
 368 variation of prediction error corresponding to different hours of day. We can find that  
 369 there are two peaks of prediction errors in 24 hours of one day. One is centered around

370 10 am, the other is around 19 pm. These two peaks are consistent with the peaking  
371 hour of public transportation. Large travel demand in Paris during the peaking hour  
372 increase the variance of Velib usage counts globally in Velib system.

## 373 6 Conclusion

374 In this paper, we aim to predict short-term Velib service demand variations at each  
375 station of Velib system based on historical Velib usage records. The simultaneously  
376 prediction for all stations is formulated as a spatio-temporal network filtering process.  
377 Given the historical Velib usage records as the input set of the network, the linkage  
378 structure of the network represents the spatio-temporal correlation structure between  
379 the historical information and the prediction target that is highly relevant with the  
380 prediction goal. A properly configured network linkage structure will give the accurate  
381 prediction efficiently. Therefore, the learning of the underlying network structure plays  
382 the key role in this work.

383 To achieve this goal, we propose to integrate a count data regression model and a  
384 sparsity-introducing regularization, named  $L1$  regularized negative binomial regression,  
385 to identify the most relevant spatio-temporal Velib usage patterns with the prediction  
386 target at each station. This procedure thus provides a sparse estimation of the network  
387 linkage structure. Due to the count data regression component, the identified linkage  
388 is designed to suit the goal of accurate temporal prediction. Benefitted from the  $L1$   
389 based sparsity regularization, the derived linkage structure is compact, in order to re-  
390 move the irrelevant and redundant information from the constructed prediction model.  
391 Experiments on massive amounts of Velib usage records in the large-scale urban area  
392 verify the superior forecast power of the proposed method. Besides, we also show that  
393 the identified spatio-temporal correlation of Velib usage records is consistent with daily  
394 Velib usage behaviors in the Velib system. This confirms the capability of the proposed  
395 method in describing the intrinsic rules of short-distance Velib travels in the city.

## 396 Acknowledgement

397 The authors wish to thank Francois Prochasson (Ville de Paris) and Thomas Valeau  
398 (Cyclocity-JCDecaux) for providing Velib data.

## 399 References

- 400 [1] APUR. Etude de localisation des stations de vlos en libre service. rapport. Tech-  
401 nical Report 349, Atelier Parisien d'Urbanisme, December 2006.
- 402 [2] P. Borgnat, C. Robardet, J.-B. Rouquier, Abry Parice, E. Fleury, and P. Flandrin.  
403 Shared Bicycles in a City: A Signal processing and Data Analysis Perspective.  
404 *Advances in Complex Systems*, 14(3):1–24, June 2011.
- 405 [3] S. Boyd and Vandenberghe. L. *Convex Optimization*. Cambridge University Press,  
406 2004.

- 407 [4] H. Bttner, J. Mlasowky, T. Birkholz, D. Groper, a.C. Fernandez, Emberger G.,  
408 and M. Banfi. Optimising bike sharing in european cities, a handbook. Technical  
409 report, Intelligent Energy Europe Program (IEE, OBIS projekt), August 2011.
- 410 [5] Yang J. C. Yan S.C. Fu Y. Cheng, B. and S. T. Huang. Learning with l1-graph  
411 for image analysis. *IEEE Transactions on Image Processing*, 19(4):858–866, 2010.
- 412 [6] B. V. Dasarathy. *Nearest neighbor (NN) norms: NN pattern classification tech-*  
413 *niques*. IEEE Computer Society Press, 1991.
- 414 [7] P. De Maio. Bike-sharing: History, impacts, models of provision, and future.  
415 *Journal of Public Transportation*, 12(4):41–56, 2009.
- 416 [8] L. Dell’Olio, A. Ibeas, and J. L. Moura. Implementing bike-sharing systems. In  
417 *ICE - Municipal Engineer*, volume 164, pages 89–101. ICE publishing, 2011.
- 418 [9] Hastie T. Friedman, J. and R. Tibshirani. Sparse inverse covariance estimation  
419 with the graphical lasso. *Biostatistics*, 9:432–441, 2008.
- 420 [10] J. Froehlich, J. Neumann, and N. Oliver. Sensing and predicting the pulse of the  
421 city through shared bicycling. In *21st International Joint Conference on Artificial*  
422 *Intelligence, IJCAI’09*, pages 1420–1426. AAAI Press, 2009.
- 423 [11] Neumann J. Froehlich, J. and Nuria. Oliver. Sensing and predicting the pulse  
424 of the city through shared bicycling. In *Proceedings of the 21st International*  
425 *Joint Conference on Artificial Intelligence*, pages 1420–1426. Morgan Kaufmann  
426 Publishers, San Francisco, USA, 2009.
- 427 [12] J. M. Hilbe. *Negative Binomial Regression: 2nd Edition*. Cambridge, 2011.
- 428 [13] Neal Lathia, A. Saniul, and L. Capra. Measuring the impact of opening the  
429 London shared bicycle scheme to casual users. *Transportation Research Part C:*  
430 *Emerging Technologies*, 22:88–102, June 2012.
- 431 [14] J.R. Lin and T. Yang. Strategic design of public bicycle sharing systems with  
432 service level constraints. *Transportation Research Part E: Logistics and Trans-*  
433 *portation Review*, 47(2):284–294, 2011.
- 434 [15] M. Meinshausen and P Buhlmann. High dimensional graphs and variable selection  
435 with the lasso. *Annals of Statistics*, 34(3), 2006.
- 436 [16] P. Vogel and D.C. Mattfeld. Strategic and operational planning of bike-sharing  
437 systems by data mining - a case study. In *ICCL*, pages 127–141. Springer Berlin  
438 Heidelberg, 2011.
- 439 [17] Ravikumar P. Wainwright, J. M. and J. D. Lafferty. High-dimensional graphical  
440 model selection using l1-regularized logistic regression. In *20th Neural Information*  
441 *Processing Systems, NIPS 2006*, Vancouver, Canada, 2006.
- 442 [18] Rutimann P. Xu M. Zhou, S.H. and P Buhlmann. High-dimensional covariance  
443 estimation based on gaussian graphical models. *Journal of Machine Learning*  
444 *Research*, 12:2975–3026, 2011.